Optical Metasurface Generated Vector Beam for Anticounterfeiting

Optical Metasurface Generated Vector Beam for Anti-counterfeiting

Chunmei Zhang, Dandan Wen, Fuyong Yue, Yuttana Intaravanne, Wei Wang*, Xianzhong Chen*

SUPA, Institute of Photonics and Quantum Sciences, School of Engineering and Physical Sciences, Heriot-Watt University, Edinburgh, EH14 4AS, UK

Abstract:

With the rapid development of optical metasurfaces, the anti-counterfeiting methods continue to evolve. Recently, the unprecedented capability of optical metasurfaces in the local manipulation of the light's polarization has been used to generate arbitrary polarization profiles, providing an unusual method for anti-counterfeiting. We experimentally demonstrate a metasurface device that can hide a quick response (QR) code in the polarization profile of a laser beam. The desired space-variant polarization profile originates from the superposition of two circularly polarized light beams with opposite handedness based on a single metasurface. A linear polarizer is used to reveal the hidden QR code. The anti-counterfeiting property of such a device has potential application in product identification, item tracking and document management.

Key words: metasurface, polarization, anti-counterfeiting, quick response code

*E-mail: w.wang@hw.ac.uk

*E-mail: x.chen@hw.ac.uk

Introduction

Hide-and-seek is a popular children's game in which some players conceal themselves in the environment, to be found by seekers. Usually a spacious place is required in order to find more hiding places for the hiders and add more difficulty for the seekers. How to play such a game in a laser beam is very challenging due to the small cross section of the laser beam. Polarization is one of the fundamental properties of a light beam, whose spatial distributions could be used to record, process and store information. However, its practical applications have been hindered by the technical challenges in the nanoscale manipulation of polarization profile even with the highest quality commercial devices. Metasurfaces are two-dimensional counterparts of metamaterials, which have drawn much attention due to their unprecedented capability in the manipulation of amplitude, phase and polarization at subwavelength scale [1-16]. Optical metasurfaces have been used to generate vector beams with typical polarization profiles (e.g, radial and azimuthal vector beams) [17] and arbitrary polarization profiles for hiding images [18, 19], providing an unusual approach for anti-counterfeiting. Quick response (QR) codes are two-dimensional barcodes consisting of usually black and white patterns with spatially varying intensity profile, which can be processed by a QR reading machine such as a smart phone. QR codes have been widely used in many fields, including product identification, item tracking and document management. To keep pace with continued miniaturization of devices and the daunting increase in the volume of information, new approaches to generate QR codes are desirable. Upon the illumination of a linearly polarized light beam, we experimentally demonstrate a metasurface device that can generate a light beam with inhomogeneous polarization profile for hiding such a QR code. Unlike recently demonstrated QR code that was encoded in the spatial amplitude modulation of a light beam generated by a metasurface [20], the QR code here is hidden in the light's polarization profile. For instance, holograms are recorded interference patterns of intensity peaks and elimination of the superimposed light wavefronts, while the QR code in our work is encoded in the inhomogeneous polarization profile of light beam with uniform intensity distribution. The reflective optical metasurface is used to generate the desired polarization distribution of the light beam. As a brand new device, its unique property may lead to wide range of applications such as anti-counterfeiting, encryption, and display.

Results and Discussion

Figure 1a shows the schematic of our proposed approach for hiding a QR code. The vector beam that can be used to hide the QR code is generated by a reflective metasurface

illuminated by a linearly polarized light beam at normal incidence. Although the resultant vector beam has a uniform intensity profile (Figure 1b), which cannot be detected by our naked eyes or cameras, it has an inhomogeneous spatial polarization profile (Figure 1c). The hidden QR code (see Figure 1d) is revealed by using a linear polarizer (analyser).

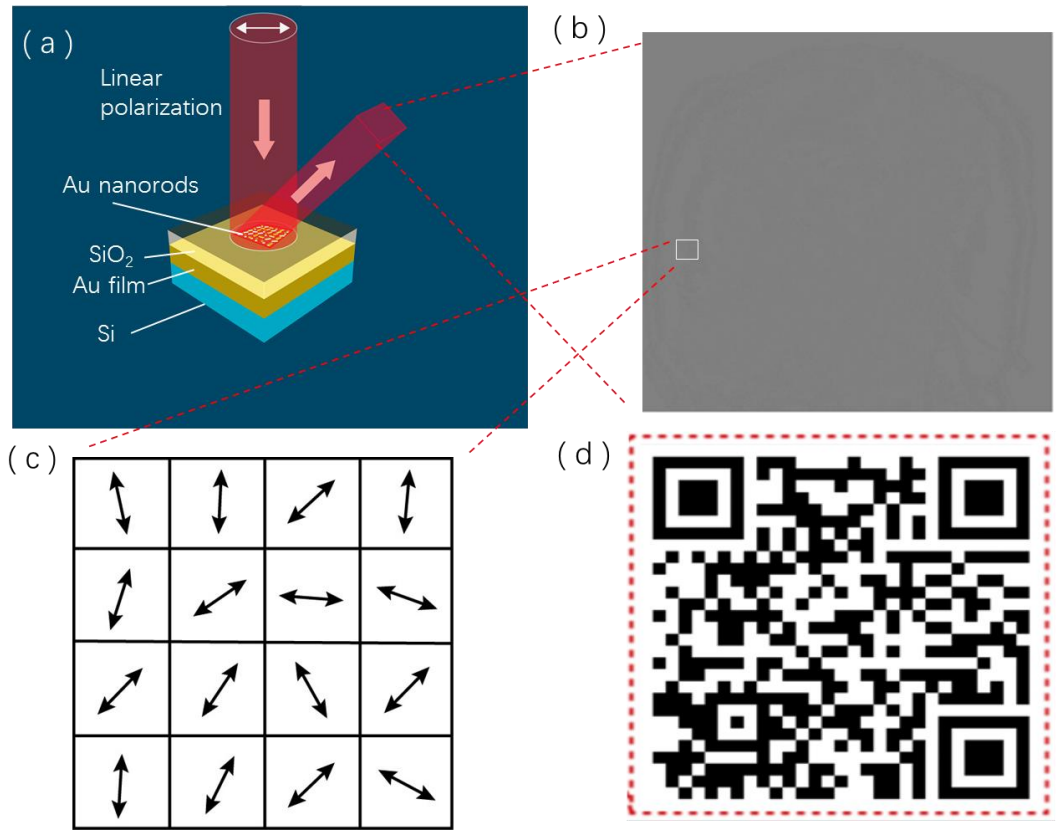

Figure 1 Schematic of the mechanism to hide a QR code in a laser beam. (a) Schematic of the design. (b) Intensity profile. (c) Schematic of polarization distribution in the white square area in (b). (d) Target QR code.

Suppose the angle between the transmission axes of the analyser and the polarizer is θ. When the completely plane polarized light from the polarizer is incident on the analyser, the electric field with an amplitude E_0 can be decomposed into two rectangular components, i.e., $E_0\cos\theta$ and $E_0\sin\theta$. However, the analyser will transmit only the component ($E_0\cos\theta$) parallel to its transmission axis. Therefore, the intensity **I** of light transmitted by the analyser is $\mathbf{I} = E_0^2\cos^2\theta$ (See Supplementary Section 1 in Ref. [21]). The desired polarization profile can be generated by a coherent superposition of two planar circularly polarized beams with opposite handedness that propagate along the same direction [8]. In order to ensure the coaxial propagation and make them interfere, a reflective metasurface is used to generate the desired

structured beams emerging from the same metasurface, which can avoid the technical hassle in the alignment system. A structured beam with an inhomogeneous polarization profile can be described as [19]

$$\boldsymbol{E}(x,y) = Aexp\big(i\theta(x,y)\big)\boldsymbol{e}_R + Bexp\big(-i\theta(x,y)\big)\boldsymbol{e}_L \quad (1)$$

where $\boldsymbol{e}_L$ and $\boldsymbol{e}_R$ are the unit vectors of left-hand circular polarization (LCP) and right-hand circular polarization (RCP). A and B denote the amplitude coefficients of RCP and LCP light, θ(x,y) represents the relative phase difference between the two orthogonal polarization states. Since the sign of the geometric phase generated at the interface of metasurface depends on the helicity of the incident light, the two beams with opposite helicity will meet and interfere with each other, generating the desired polarization profile for the hidden QR code. Different from a common polarized laser beam, which typically has only one polarization state, different parts of the beam here have spatially variant polarization states.

The generation of desired polarization profiles with two opposite handedness and their superposition process occur on the same metasurface by controlling the polarization state of the incident light. Detailed information is available in Supplementary Section 2 [21]. To maintain high efficiency and broadband, we leverage the recent advances in the realization of high efficiency, broadband reflective-type configuration and Pancharatnam-Berry phase metasurface to develop the designed metasurface device. Compared to other types of metasurfaces, a metasurface consisting of nanorods with spatially varying orientation shows superior in phase control for the circular polarization and can ease the fabrication. The three-layer structure functions like a Fabry-Pérot–like cavity, where the thickness of the SiO_2 spacer corresponds to the cavity length. Nanorod along with the spacer and the background layer function as a reflective-type half-wave plate. Detailed theoretical analysis of the broadband characteristic of such metasurfaces is available in the references [22, 23]. The reflective metasurface consists of three layers: gold nanorods on the top (30 nm), a gold layer at the bottom (150 nm) and a silicon dioxide (SiO_2) spacer layer (85 nm) sandwiched between them. All the nanorods have same geometry with various orientation angles. Each nanorod corresponds to a pixel, which has a dimension of 300 nm by 300 nm, indicating the subwavelength resolution. Each nanorod is 200 nm long, 50 nm wide and 30 nm high. To generate the off-axis reflection (See Supplementary Section 3 in Ref. [21]), the additional phase difference between neighboring pixels of the sample to along x direction is $\pi/5$, resulting in a reflection angle of 12.2^o at the incident wavelength of 650 nm. The standard electron-beam lithography is used to fabricate the designed metasurface, followed by the lift-

off process. For the adhesion purpose, a thin titanium layer (3 nm) is deposited on the SiO2 layer prior to the layer for the gold nanorods. Fabrication details are available in the Supplementary Section 4 [21]. The metasurface device has a dimension of 300 μm by 300 μm. Fig.2a shows the SEM image of the metasurface. In order to visualize the hidden QR code, an analyser is used to reveal the hidden information in the polarization topology of the laser beam. In doing so, we do not directly observe the spatially-variant polarization profile of the laser beam but rather indirectly confirm its existence through the intensity profile behind the analyser and the interference fringes resulted from the right and left circular components. The experimental setup used to characterize the fabricated sample is shown in Fig.2b.

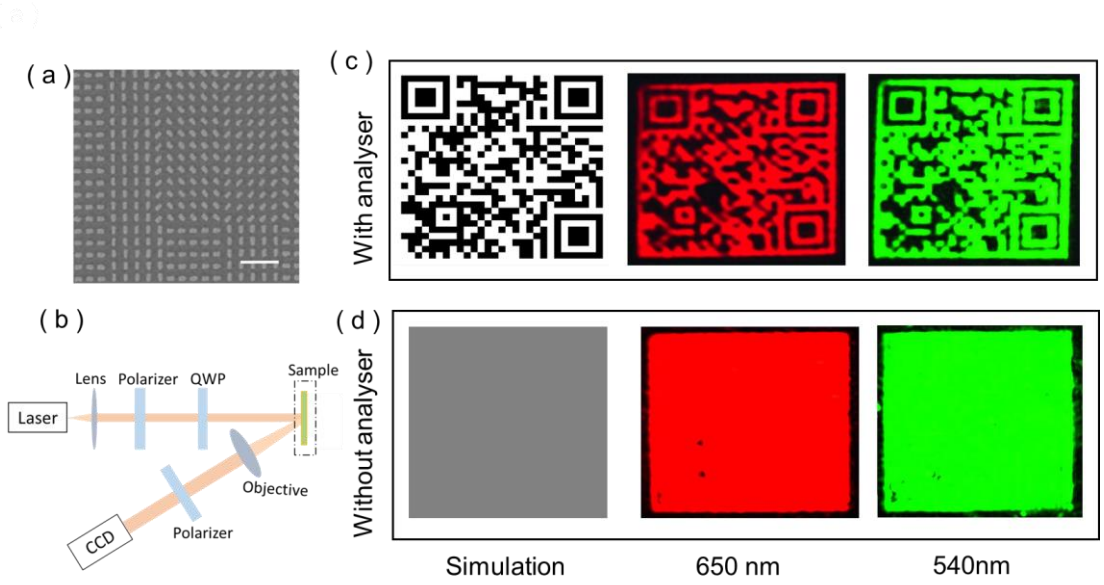

Figure 2 Simulation and experimental results. (a) SEM image of the fabricated sample. The scale bar is 1 μm. The size of fabricated sample is 300 μm by 300 μm. Each unit cell is 300 nm by 300 nm. (b) Schematic of experimental setup. QWP: quarter waveplate. Simulation and experimental results (c) with and (d) without the analyser.

Fig.2b is the schematic of experimental setup. To characterize the performance of the active metasufaces, a tunable laser source (NKT-SuperK EXTREME) is used to generate the desired laser beam with various polarization states after passing through a quarter-wave plate (QWP) and a polarizer in front of the sample (see Supplementary Section 5 in Ref. [21]). An objective with a magnification of 10× is used to expand the image for visualization with a charge-coupled device (CCD) camera. Fig.2c and 2d show the simulation and experimental results with and without analyser under the illumination of linearly polarized light beams.

The figures in Fig.2c and Fig.2d on the left, middle and right columns represent the simulation results and experimental results at 650 nm and 540 nm, respectively. The slight difference between experiment and simulation is due to the imperfection of the sample and measurement error. Although the device is designed at the operating wavelength of 650 nm, it can operate in a broad wavelength range due to the broadband nature of the geometric metasurface. The experimental results at 540 nm (see right column of Fig.2c and Fig.2d) are given as well. The QR code contains the information of our group website (http://nanophotonicslab.eps.hw.ac.uk/), which can be accessed by using QR code reader such as a smart phone. Due to the off-axis design, another identical image is also observed in the reflected beam on the other side with respect to the surface normal.

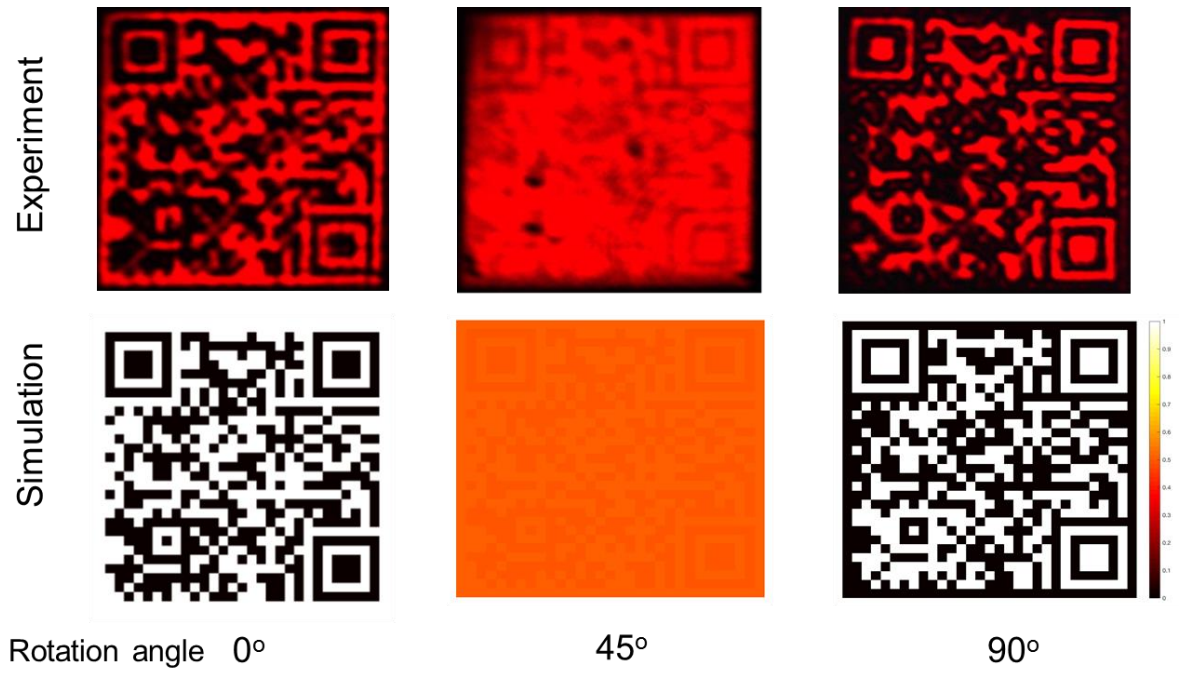

Figure 3 The dependence of experimental results on the rotation angles of the transmission axis of the analyser away from the vertical direction. The incident light is linearly polarized along the horizontal direction.

We further characterize the device by studying the relationship between the obtained QR code images and the transmission axis of the analyser. It is worth mentioning that the transmission axes of the polarizer (before the sample) and the analyser (after sample) are designed along the horizontal and vertical directions, respectively. Various QR codes are obtained by rotating the transmission axis of the analyser (designed along the vertical direction), while that of the polarizer is fixed along the horizontal direction. Fig.3 shows the

simulation and experimental results when the rotation angles of the analyser (away from the designed direction) are 0, π/4, and π/2, respectively. Interestingly, the two QR codes for the analyser with orthogonal directions of transmission axis (0 and π/2) are complementary images, i.e., the brightest area becomes the darkest area and vice versa. The complementary images by changing transmission axis of the analyser can be explained by using Malus' law. Suppose the angle distribution between the transmission axes of the analyzer and the polarization profile of the light beam reflected by the metasurface device is $\beta(x, y)$, then the intensity of the light passing through the analyzer with a transmission axis along horizontal direction is $I_0 cos^2 \beta(x, y)$, where I_0 is the intensity of incident light. After rotating the analyser by 90 degrees, the transmitted light intensity distribution will be $I_0 cos^2 \left[\beta(x, y) + \frac{\pi}{2}\right] = I_0[1 - cos^2 \beta(x, y)]$. The hidden target QR code can hardly be observed when the rotation angle is π/4.

Next, the dependence of experimental results on the incident polarization state is investigated. Although our design is based on the incident light with linear polarization, the experimental results for other polarization states are also obtained. Various polarization states are generated by controlling the angle between the transmission axis (fixed along the *x* direction) of a linear polarizer and the fast axis of a quarter waveplate. Fig.4 shows the simulation and experimental results for the incident light with linear polarization and elliptical polarization, respectively. Simulation results for other polarization states are provided in the Supplementary Section 5 [21]. Obviously, the image contrast is deteriorated when incident polarization state is away from the desired one (linear polarization). Furthermore, the generated QR code in Fig.4 (b) doesn't work anymore due to the low image contrast.

Although the metasurface approach has been used to generate arbitrary polarization profile [18, 19], the generated QR codes with unique property are very attractive and potentially useful for both anti-counterfeiting and encryption. Despite the broadband nature the reflective metasurface, the developed device cannot operate under the illumination of white light sources since there is a slight change of the off-axis reflection at different wavelengths. The device here is demonstrated based on reflective metasurface, but the dielectric metasurface [24] can make it work in the transmission mode, which is more compatible with most optical systems. QR codes embedded in the polarization profile of a light beam are very difficult to counterfeit due to the specialized and technologically advanced process (precise polarization

control) and equipment (e.g., electron beam lithography). The simple decoding process (with a linear polarizer) can meet the verification requirement of fast speed and simplicity, which can speed up the processing of QR codes by a QR code reading machine.

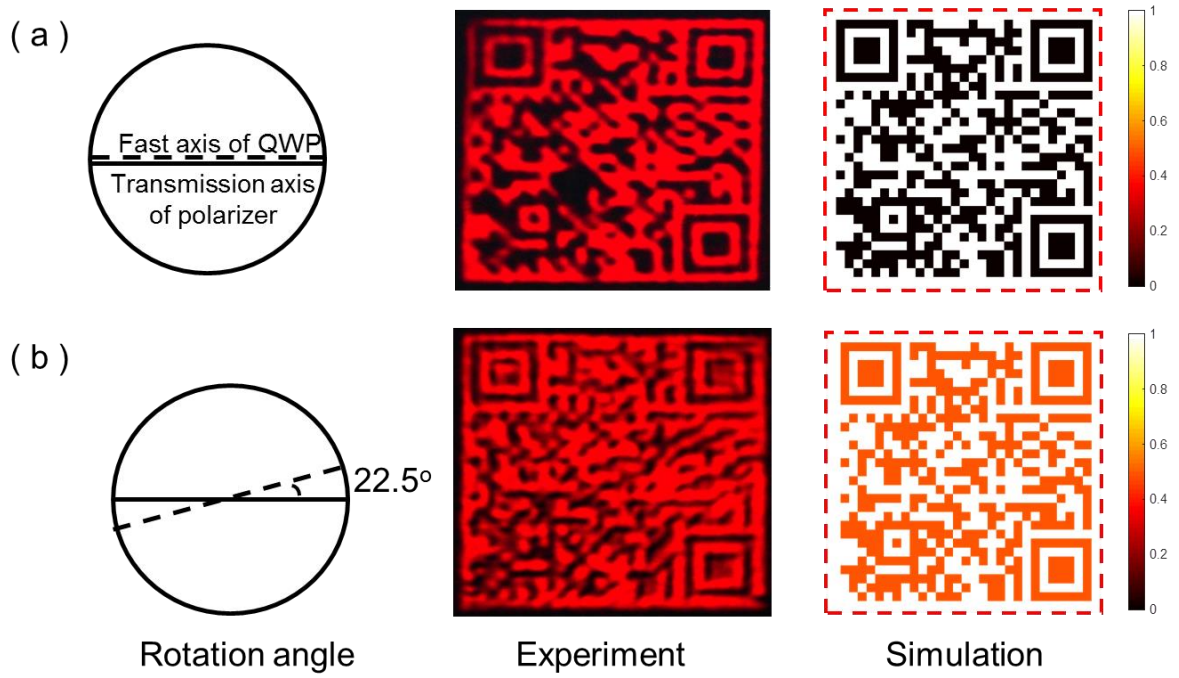

Figure 4 The dependence of experimental results on polarization states of incident light. The angles between the transmission axis (fixed along the horizontal direction) of a linear polarizer and the fast axis of the quarter waveplate (QWP) are 0 and $\pi/8$, respectively.

In summary, we experimentally demonstrate a metasurface device that can encode a QR code in the polarization profile of a laser beam. These hidden QR codes demonstrate the rich structure of a generated light beam by an optical metasurface that can possess at subwavelength scales. The unique measurement technique used here holds great promise for anti-counterfeiting and encryption, which have potential application in product identification, item tracking and document management.

Acknowledgments

X.C. acknowledges the Engineering and Physical Sciences Research Council of the United Kingdom (Grant Ref: EP/ P029892/1).

References:

[1] N. Yu, P. Genevet, M. A. Kats, F. Aieta, J. P. Tetienne, F. Capasso and Z. Gaburro, Light Propagation with Phase Discontinuities: Generalized Laws of Reflection and Refraction, Science 334, 333(2011).

[2] X. Ni, N.K. Emani, A.V. Kildishev, A. Boltasseva and V.M. Shalaev, Broadband light bending with plasmonic nanoantenas, Science 335, 427(2012).

[3] L. Huang, X. Chen, H. Mühlenbernd, G. Li, B. Bai, Q. Tan, G. Jin, T. Zentgraf and S. Zhang, Dispersionless Phase Discontinuities for Controlling Light Propagation, Nano Lett 12, 5750(2012).

[4] S. Sun, Q. He, S. Xiao, Q. Xu, X. Lin and L. Zhou, Gradient-index meta-surfaces as a bridge linking propagating waves and surface waves, Nat. Mater. 11, 426(2012).

[5] X. Yin, Z. Ye, J. Rho, Y. Wang and X. Zhang, Photonic Spin Hall Effect at Metasurfaces, Science 339, 1405(2013).

[6] X. Chen, L. Huang, H. Mühlenbernd, G. Li, B. Bai, Q. Tan, G. Jin, C. Qiu, S. Zhang and T. Zentgraf, Dual-Polarity Plasmonic Metalens for Visible Light, Nat. Commun. 3, 1198(2012).

[7] G. Zheng, H. Mühlenbernd, M. Kenney, G. Li, T. Zentgraf and S. Zhang, Metasurface holograms reaching 80% efficiency, Nat. Nanotechnol. 10, 308(2015).

[8] F. Yue, D. Wen, C. Zhang, B. D. Gerardot, W. Wang, S. Zhang, and X. Chen, Multichannel Polarization-Controllable Superpositions of Orbital Angular Momentum States, Adv. Mater. 29, 1603838(2017).

[9] C. Zhang, F. Yue, D. Wen, M. Chen, Z. Zhang, W. Wang and X. Chen, Multichannel metasurface for simultaneous control of holograms and twisted light beams, ACS Photonics 4, 1906(2017).

[10] F. Yue, X., Zang, D. Wen, Z. Li, C. Zhang, H. Liu, B.D. Gerardot, W. Wang, G. Zheng and X.Chen, Geometric Phase Generated Optical Illusion, Sci. Rep. 7, 11440(2017).

[11] D. Wen, F. Yue, C. Zhang, X. Zang, H. Liu, W. Wang and X. Chen, Plasmonic metasurface for optical rotation, Appl. Phys. Lett. 111, 023102(2017).

[12] J. Burch, D. Wen, X. Chen and A.D. Falco, Conformable Holographic Metasurfaces, Sci. Rep. 7, 4520(2017).

[13] D. Wen, F. Yue, M. Ardron and X. Chen, Multifunctional metasurface lens for imaging and Fourier transform, Sci. Rep. 6, 27628(2016).

[14] X. Chen, Y. Zhang, L. Huang and S.Zhang, Ultrathin metasurface laser beam shaper, Adv. Opt. Mater. 2, 978(2014).

[15] G. Li, S. Zhang and T. Zentgraf, Nonlinear photonic metasurfaces, Nat. Rev. Mater. 2, 17010(2017).

[16] D. Hu, X. Wang, S. Feng, J. Ye, W. Sun, Q. Kan, P. J. Klar and Y. Zhang, Ultrathin terahertz planar elements, Adv. Opt. Mater. 1, 186(2013).

[17] F. Yue, D. Wen, J. Xin, B. D. Gerardot, J. Li and X. Chen, Vector vortex beam generation with a single plasmonic metasurface, ACS Photon. 3, 1558(2016).

[18] L. Wang, T. Li, R. Guo, W. Xia, X. Xu and S. Zhu, Active display and encoding by integrated plasmonic polarizer on light-emitting-diode, Sci. Rep. 3, 2603(2013).

[19] F. Yue, C. Zhang, X. Zang, D. Wen, B.D. Gerardot, S. Zhang and X. Chen, High-resolution grayscale image hidden in a laser beam, Light: Sci. Appl. 7, e17129(2018).

[20] A. Chanana, A. Paulsen, S. Guruswamy and A. Nahata, Hiding multi-level multi-color images in terahertz metasurfaces, Optica 3, 1466(2016).

[21] See Supplemental Material at [URL will be inserted by publisher] for further details of Malus' law, polarization profile generation, off-axis reflection design, fabrication procedure of the metasurface and generation of incident light with various polarization states.

[22] S. Jiang, X. Xiong, P. Sarriugarte, S. Jiang, X. Yin, Y. Wang, R. Peng, D. Wu, R. Hillenbrand, X. Zhang and M. Wang, Tuning the polarization state of light via time retardation with a microstructured surface, Physical Review B 88, 161104(2013).

[23] D. Wen, F. Yue, G. Li, G. Zheng, K. Chan, S. Chen, M. Chen, K.F. Li, P. W. Wong, K.W. Cheah, E.Y. Pun, S. Zhang and X. Chen, Helicity multiplexed broadband metasurface holograms, Nat. Commun. 6, 8241(2015).

[24] S. Kruk, B. Hopkins, I.I. Kravchenko, A. Miroshnichenko, D. Neshev and Y. Kivshar, Invited Article: Broadband highly efficient dielectric metadevices for polarization control, APL Photonics *1*, 030801(2016).